

DOI: 10.1002/cmdc.201402007

Photodelivery of CO by Designed PhotoCORMs: Correlation between Absorption in the Visible Region and Metal–CO Bond Labilization in Carbonyl Complexes

Indranil Chakraborty, Samantha J. Carrington, and Pradip K. Mascharak*^[a]

The therapeutic potential of photoactive CO-releasing molecules (photoCORMs) have called for close examination of the roles of the ligand(s) and the central metal atoms on the overall photochemical labilization of the metal–CO bonds. Along this line, we have synthesized four metal complexes, namely, [MnBr(azpy)(CO)₃] (**1**), [Mn(azpy)(CO)₃(PPh₃)ClO₄] (**2**), [ReBr(azpy)(CO)₃] (**3**), and [Re(azpy)(CO)₃(PPh₃)ClO₄] (**4**), derived from 2-phenylazopyridine. These complexes were characterized by spectroscopic and crystallographic studies. Although both **1** and **3** exhibit strong metal-to-ligand charge-transfer bands in

the 500–600 nm region, only **1** photoreleases CO upon illumination with visible light. Results of theoretical studies were used to gain insight into this surprising difference. Strong spin-orbit coupling (prominent in heavy metals) appears to promote intersystem crossing to a triplet state in **3**, a step that discourages CO release upon illumination with visible light. Slow release of CO from **2** and **4** also indicates that strong σ -donating ligands, such as Br[−], accelerate the rate of CO photo-release relative to π -acid ligands, such as PPh₃.

Introduction

The deleterious effects of carbon monoxide (CO) observed in mammalian physiology arise from its strong affinity to heme centers in proteins. Binding of CO to hemoglobin leads to asphyxia, an effect that has earned this diatomic molecule the moniker of “silent killer”. However, CO is produced endogenously through heme degradation by the heme oxygenase (HO) enzyme^[1] and in low doses, CO has recently been shown to impart beneficial effects in various physiological pathways, including vasorelaxation. More surprisingly, low doses of CO exhibit anti-inflammatory and anti-apoptotic properties.^[2,3] As a consequence, CO provides protection to oxidatively damaged tissues, such as in ischemic reperfusion injury and endothelial impairment during balloon angioplasty. It is therefore expected that CO could play a crucial role as a therapeutic agent in cardiovascular disease and organ transplantation protocols.^[4] In addition, Motterlini et al. have shown that, although CO induces an anti-apoptotic effect in endothelial cells, it can impart considerable pro-apoptotic effects in hyperproliferative tissues.^[2] Collectively, these findings have prompted considerable research effort in recent times to use CO as a chemotherapeutic in various settings.^[2,3] However, administration of CO in gaseous form raises serious issues in terms of controlled and safe delivery to biological targets. To circumvent these obstacles, various research groups have directed their efforts to develop suitably designed metal–carbonyl complexes^[5–7] as CO-

releasing molecules (CORMs) to deliver CO in a more controlled fashion. The major drawbacks of such first-generation CORMs are associated with their solubility and stability under ambient conditions.^[2,8] Air-stable and water-soluble metal–carbonyls, such as [Re(CO)₃(H₂O)₃]⁺ and [Tc(CO)₃(H₂O)₃]⁺, show no reactivity in terms of CO release,^[9] and in cases of amino acid-derived carbonyl complexes such as [RuCl(gly)(CO)₃] (CORM-3), solvent-assisted CO release is triggered through hydrolysis, and a significantly shortened half-life under specific physiological conditions inhibits sustained delivery of CO to desired targets.^[8b,c]

During the past few years, the photo-induced CO-releasing molecules (photoCORMs) have emerged as credible alternatives.^[10–12] Here, the CO release from the metal–carbonyl complexes (which are otherwise stable under dark conditions) can be achieved through exposure to light. In earlier attempts, typical carbonyls such as [Mn₂(CO)₁₀] and [Fe(CO)₅] were used for photodelivery of CO.^[13] Unfortunately, high toxicity and lack of chemical amenability restricted their applicability in biological systems. In recent years, several research groups have developed suitably designed photoCORMs based on transition metal–carbonyls to alleviate such limitations.^[11,12] For example, the rhenium-based water-soluble photoCORM [Re(bpy)(CO)₃-(thp)]⁺ (thp = tris(hydroxymethyl)phosphine), developed by Ford and co-workers, is readily internalized by human prostatic carcinoma cells with no apparent cytotoxicity.^[14] When the loaded cells are irradiated with UV light (405 nm), CO release can be visualized by a change in fluorescence. Schatzschneider and co-workers have synthesized the cationic [Mn(CO)₃(tpm)]⁺ (tpm = tris(pyrazolyl)methane) complex that initiates photodelivery of CO upon illumination with UV light (365 nm).^[15] This photoCORM has been shown to eradicate human colon cancer

[a] Dr. I. Chakraborty, S. J. Carrington, Prof. P. K. Mascharak
Department of Chemistry and Biochemistry
University of California Santa Cruz
1156 High Street, Santa Cruz, CA 95064 (USA)
E-mail: pradip@ucsc.edu

 Supporting information for this article is available on the WWW under <http://dx.doi.org/10.1002/cmdc.201402007>.

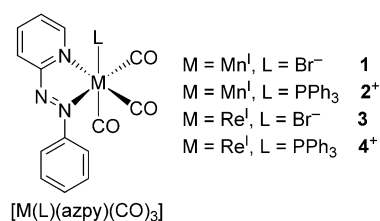
cell (HT29) through efficient internalization and CO delivery. The development of designed photoCORMs, however, faces the major challenge of synthesizing suitable metal–carbonyl complexes that can liberate CO upon irradiation with light in the biocompatible range (500–900 nm).^[12] To date, the vast majority of photoCORMs have shown sensitivity toward UV light (300–450 nm),^[11,12,16–22] an untenable range of wavelengths in terms of developing phototherapeutics, with very few exceptions.^[23–25]

In our attempt to correlate the light absorption parameters of designed metal–carbonyl complexes with their ability to photorelease CO, we looked at various ligands that give rise to carbonyl complexes with varying numbers of CO ligands.^[16,25] In our recent effort, we selected the ligand 2-phenylazopyridine (azpy), which resembles α,α' -diimine ligands such as bipyridine (bpy) and *ortho*-phenanthroline (*o*-phen). Metal–carbonyl complexes derived from these α,α' -diimine ligands have recently been employed as photoCORMs by different groups.^[11,12,14] In a previous communication, we reported a very efficient Mn-based photoCORM, namely, *fac*-[MnBr(azpy)(CO)₃] (**1**), which rapidly releases CO (quantum yield $\varphi = 0.48$) upon illumination with low-power visible light.^[23] Moreover, CO liberated from this complex has been used to inflict severe damage to HeLa and MDA-MB-231 cancer cells. The phosphine-substituted complex *fac*-[Mn(azpy)(CO)₃(PPh₃)]ClO₄ (**2**) also exhibits sensitivity to visible light. To further increase the stability of this type of photoCORMs in biological media, we have now synthesized the corresponding rhenium complexes, *fac*-[ReBr(azpy)(CO)₃] (**3**) and *fac*-[Re(azpy)(CO)₃(PPh₃)]ClO₄ (**4**), and examined their CO-releasing properties. As both of these complexes display strong absorption bands in the visible (~500 nm) region, analogous to their Mn progenitors, we expected that the associated metal-to-ligand charge transfer (MLCT) transitions would augment CO release. However, both **3** and **4** release CO only upon illumination with UV light. In addition, the rates of CO release from **3** and **4** are significantly slower than from the corresponding Mn complexes **1** and **2**. Clearly, these findings raise the critical question of why the structurally and electronically similar rhenium carbonyl complexes fail to photorelease CO upon exposure to visible light, despite strong absorption in the visible region. To explore the cause of discrepancy in light sensitivity between **1** and **3** (derived from metal centers with same low-spin d⁶ configuration), we performed density functional theory (DFT) and time-dependent density functional theory (TDDFT) calculations on **1–4**. The results, as described in this article, reveal for the first time the role of transition metal centers (within the same group) on the CO-releasing capacities of structurally identical complexes. It is now evident that judicious choice of the metal center, along with proper combination of ligand/co-ligand, are critical to achieve the objective of CO delivery under the control of visible/near-IR light.

Results and Discussion

Synthesis

Reaction of [MnBr(CO)₃] with one equivalent of azpy ligand in dichloromethane at room temperature afforded the *fac*-[MnBr(azpy)(CO)₃] (**1**) complex. During the synthesis, the entire reaction setup was properly covered with aluminum foil to protect from exposure to ambient light source. The Re analogue *fac*-[ReBr(azpy)(CO)₃] (**3**) was synthesized by reacting [ReBr(CO)₃] with one equivalent of azpy ligand in boiling benzene. Previously, Ishitani and co-workers showed that incorporation of a π -acceptor ligand like PPh₃ in metal–carbonyl complexes enhances the rate of CO release.^[26] In such species, competition between PPh₃ and the *trans* CO group for the same π -symmetry orbital causes CO labilization. We therefore undertook the task of synthesizing the phosphine complexes through replacement of the bromide group of **1** and **3**. The *fac*-[Mn(azpy)(CO)₃(PPh₃)]ClO₄ (**2**) complex was synthesized in two steps. Complex **1** was first stirred with one equivalent of AgClO₄ in tetrahydrofuran (THF), and the resulting AgBr was removed by filtration. Following removal of THF, one equivalent of PPh₃ in dichloromethane was added to the residue (presumably the [Mn(azpy)(CO)₃(THF)]ClO₄ complex), and the mixture was stirred at room temperature for an extended period to isolate **2**. In the case of *fac*-[Re(azpy)(CO)₃(PPh₃)]ClO₄ (**4**), both steps were carried out at reflux in THF and chloroform, respectively. The general structures of **1–4** are depicted in Scheme 1.



Scheme 1. Manganese and rhenium carbonyl complexes reported herein.

To analyze the effect of the azpy ligand, we also synthesized *fac*-[MnBr(bpy)(CO)₃] and *fac*-[ReBr(bpy)(CO)₃] by following procedures developed in our laboratory (see below).

X-ray structures

Dark, block-shaped crystals of **1** and **3** and orange needles of **2**, **4**, and *fac*-[MnBr(bpy)(CO)₃] were obtained by layering hexanes over their solution in dichloromethane. We reported the structures of **1** and **2** in a previous communication.^[23] The structures of complexes **3** and **4** with atom labeling are shown in Figures 1 and 2. Selected metric parameters of **3** and **4** are listed in Table 1. Complete crystal structure determination and refinement parameters for **1–4** (Table S1), metric parameters for **1** and **2** (Table S2), and crystal and metric parameters for *fac*-[MnBr(bpy)(CO)₃] (Table S3) are available in the Supporting Information.

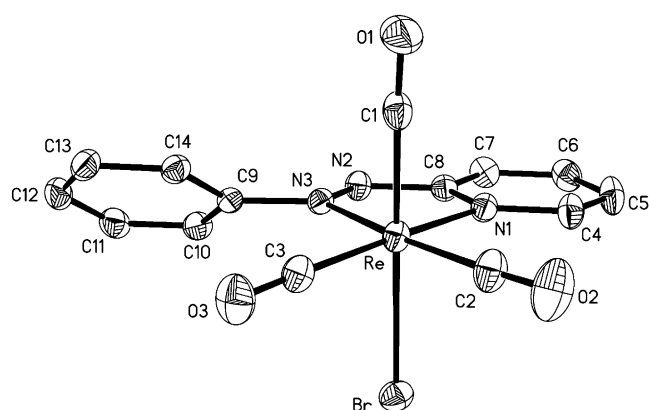


Figure 1. Molecular structure of *fac*-[ReBr(azpy)(CO)₃] (**3**). Thermal ellipsoids are shown at 50% probability level, with the hydrogen atoms omitted for clarity.

Table 1. Selected bond distances [Å] and angles [°].		
Bond	<i>fac</i> -[ReBr(azpy)(CO) ₃] (3)	<i>fac</i> -[Re(azpy)(CO) ₃ (PPh ₃)]ClO ₄ (4)
Re–N1	2.149(3)	2.1511(18)
Re–N3	2.156(3)	2.1588(19)
Re–C1	1.922(4)	1.967(3)
Re–C2	1.920(4)	1.931(2)
Re–C3	1.929(4)	1.936(2)
Re–Br	2.6217(5)	–
Re–P1	–	2.5199(6)
N2–N3	1.271(4)	1.277(3)
C2–Re–C1	87.79(16)	87.65(10)
C2–Re–C3	87.82(15)	90.77(10)
C1–Re–C3	90.63(15)	91.25(10)
C2–Re–N1	97.94(13)	94.57(9)
C3–Re–N1	172.37(12)	174.66(8)
C1–Re–N1	94.57(13)	88.82(9)
C2–Re–N3	170.74(13)	167.18(9)
C3–Re–N3	101.27(12)	101.89(9)
C1–Re–N3	93.84(13)	94.05(9)
N1–Re–N3	72.85(10)	72.78(7)
C1–Re–Br	179.33(11)	–
C2–Re–Br	92.30(12)	–
C3–Re–Br	90.04(11)	–
N1–Re–Br	84.75(7)	–
N3–Re–Br	85.96(7)	–
C2–Re–P1	–	88.90(8)
C3–Re–P1	–	88.38(7)
C1–Re–P1	–	176.53(8)
N1–Re–P1	–	91.87(5)
N3–Re–P1	–	89.40(5)

The coordination geometry of the Mn and Re centers in **1–4** is distorted octahedral, and the three CO ligands are facially disposed. The two nitrogen atoms of the azpy ligand and the two carbon atoms from the CO groups constitute the equatorial plane, while the axial positions are occupied by a CO group and Br[–] or PPh₃. In all of the structures, the N–N distances of the azo group are uniformly longer than that of the uncoordinated 2-phenylazopyridine ligand (1.25(3) Å).^[27] This lengthening indicates strong d(Mn/Re)→azo(π*) back-bonding character in the present complexes. Careful scrutiny of the metric parameters of **1**^[23] with the structurally similar *fac*-[MnBr-

(bpy)(CO)₃] reveals certain differences. The Mn–C2 distance in **1** is 1.8139(18) Å, which is noticeably longer than the average of Mn–C2 distances in *fac*-[MnBr(bpy)(CO)₃] (1.803(4) Å). This weakening can be attributed to the superior π-acidity of the azo group^[28] *trans* to the Mn–C2 bond in **1**. In contrast, the Re–C2 distance in **3** (1.920(4) Å) is slightly shorter than the average of the corresponding distances in the structurally similar *fac*-[ReBr(Me₂bpy)(CO)₃] (1.925(3) Å).^[29] Similarly, the Re–C2 distance in **4** (1.931(2) Å) is slightly shorter than the average of the corresponding distances in *fac*-[Re(bpy)(CO)₃(PPh₃)]⁺ (1.939(16) Å) (Figure 2).^[30] These structural characteristics sug-

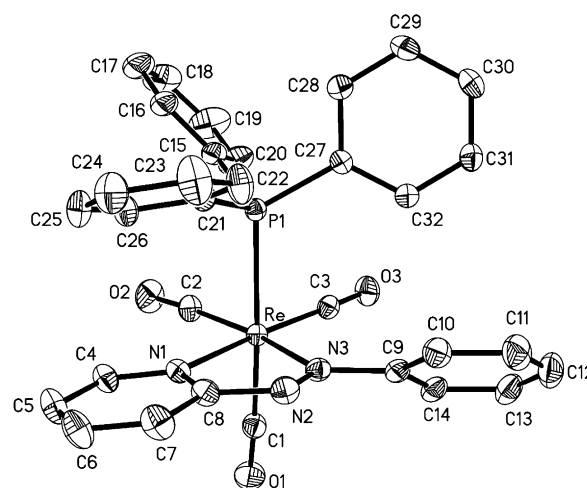


Figure 2. Molecular structure of the cation of *fac*-[Re(azpy)(CO)₃(PPh₃)]ClO₄ (**4**). Thermal ellipsoids are shown at 50% probability level, with the hydrogen atoms omitted for clarity.

gest that the *trans* effect of the azo group is not prominent in rhenium complexes. Comparison of the metal–N distances of **1–4** with the corresponding bpy complexes also indicates that the azpy ligand binds the metal centers more strongly than the bpy/Me₂bpy ligand in the corresponding complexes. Once again, this can be ascribed to the superior π-acceptor character of the azpy ligand, which is well-suited for binding the low-valent low-spin d⁶ metal centers in **1–4**.

Spectroscopic properties

The three facially disposed CO ligands in all of the complexes gave rise to νCO bands in the expected regions (2030, 1930, 1920 cm^{–1} for **3**; 2050, 1970, 1940 cm^{–1} for **4**). In addition, the ν_{N=N} stretch was observed near 1370 cm^{–1} for all of the complexes. All complexes display ¹H NMR spectra consistent with the diamagnetic ground state of the Re^I and Mn^I centers (example shown in Figure 3).

Solutions of the complexes in methanol, chloroform, dichloromethane, and acetonitrile are indefinitely stable in the absence of light. The complexes are also stable under aerobic conditions, which is important for biological compatibility and controlled release of CO. The electronic absorption spectra of the complexes consist of two bands. One of the bands appears

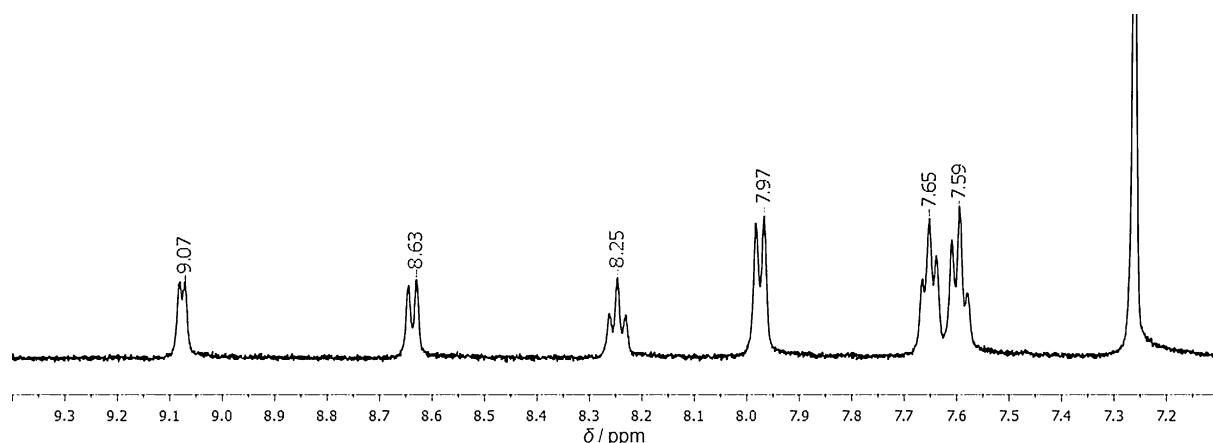


Figure 3. ^1H NMR spectrum of $[\text{ReBr}(\text{azpy})(\text{CO})_3]$ (**3**) in CDCl_3 solution at 298 K.

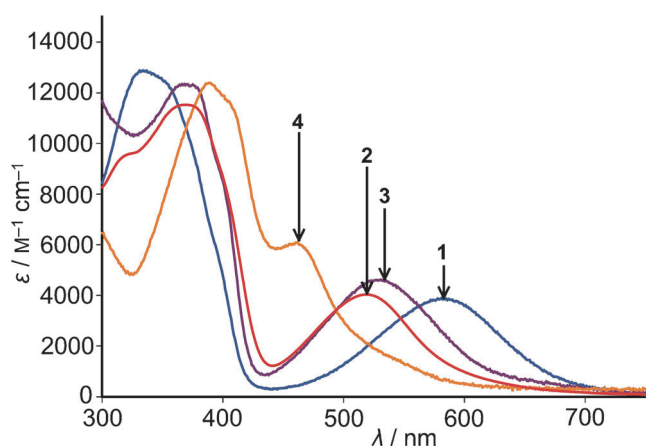


Figure 4. Electronic absorption spectra of **1–4** in dichloromethane.

in the range 330–390 nm, while the absorption maxima of the second band span a range of 460–590 nm (Figure 4). The latter absorption is likely to arise from the MLCT ($\text{metal}(d\pi) \rightarrow \text{azo}(\pi^*)$) transition, with considerable XLCT ($\text{halide}(p) \rightarrow \text{azo}(\pi^*)$) contributions for **1** and **3** (see below). A close inspection of the electronic absorption spectra of **1** and **3** reveals the effect of replacement of the group 7 d^6 metal center. Complex **1** displays a dark royal blue color in dichloromethane solution (MLCT band at 586 nm). Replacement of the Mn center with Re^I in **3** results in a blue shift of the MLCT band to 530 nm (Figure 4), and the color of the dichloromethane solution changes to deep purple. It is important to note that the lower energy bands are highly blue shifted in **2** and **4** relative to **1** and **3**. The PPh_3 ligand (a good π -acceptor) in these complexes draws more electron density from the metal center and stabilizes the highest-occupied orbitals. Such stabilization increases the energy of the MLCT transitions and causes the blue shift observed with **2** and **4**.

Photorelease of CO from **1–4**

Manganese complexes **1** and **2** exhibit excellent photoactivity upon exposure to low-power visible light ($10\text{--}15 \text{ mW cm}^{-2}$).^[23] Such illumination causes rapid changes in the absorption spectra due to loss of CO, and distinct isosbestic points indicate the clean conversion of the complexes to their corresponding photo products. Photorelease of CO has been confirmed in these photolytic processes by standard myoglobin (Mb) assay. Results of a representative Mb assay are shown in Figure 5.

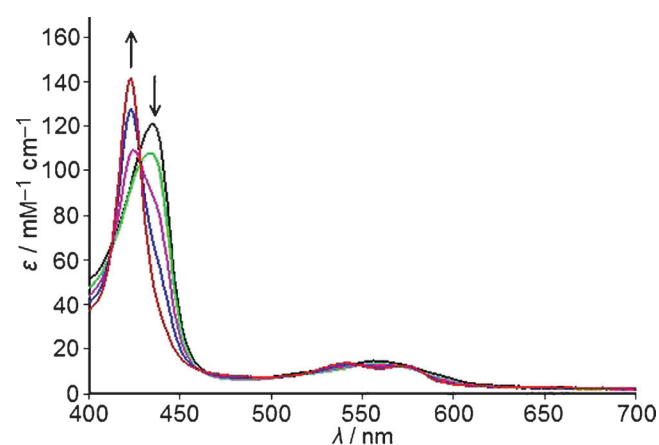


Figure 5. UV/Vis traces from the myoglobin (Mb) assay for **2**. Formation of the Mb–CO adduct from reduced Mb is evident by the shift in the Soret band from 435 to 424 nm.

The rates of CO photorelease (k_{CO}) from all four complexes were determined spectrophotometrically. In dichloromethane, **1** and **2** exhibited k_{CO} values of $21.94 \pm 0.01 \text{ min}^{-1}$ (conc.: $1.23 \times 10^{-4} \text{ M}$) and $15.28 \pm 0.01 \text{ min}^{-1}$ (conc.: $3.07 \times 10^{-4} \text{ M}$), respectively, upon illumination with visible light. In contrast, photorelease of CO from **3** and **4** could only be initiated by exposure to low power UV light (centered at 305 nm, 5 mW cm^{-2}) despite strong MLCT bands in the 430–530 nm region. Exposure to UV light also resulted in distinct isosbestic points in their absorption spectra, suggesting clean conversions

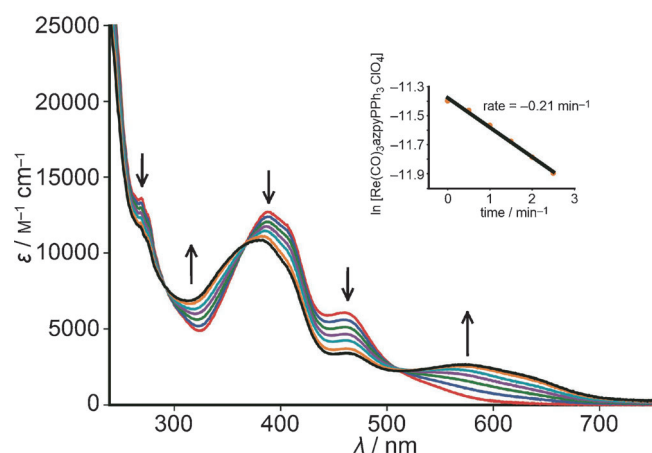


Figure 6. Changes in the electronic absorption spectrum of **4** in dichloromethane solution upon exposure to UV light (5 mW cm^{-2}). The inset displays the k_{CO} rate plot for complex **4**.

(Figure 6), and the rates of CO photorelease were similar. For example, in dichloromethane, **3** and **4** exhibited k_{CO} rates of $0.25 \pm 0.01 \text{ min}^{-1}$ (conc.: $1.26 \times 10^{-4} \text{ M}$) and $0.21 \pm 0.01 \text{ min}^{-1}$ (conc.: $6.94 \times 10^{-5} \text{ M}$), respectively.

Light-induced loss of CO from structurally similar bpy complexes has been reported by several groups.^[31] Close scrutiny of the results reveals that the structurally similar *fac*-[MnBr(bpy)(CO)₃] displays its most red-shifted MLCT band at 420 nm. When we exposed this complex to 420 nm light, spectral changes due to CO photorelease were also observed. The rate of CO photorelease, however, was slower ($1.21 \pm 0.01 \text{ min}^{-1}$, conc.: $1.15 \times 10^{-4} \text{ M}$) than that noted with **1** (Figure S9, Supporting Information). Faster CO release was observed when this complex was irradiated with UV light ($\sim 300\text{--}325 \text{ nm}$). In dichloromethane, the k_{CO} rate of *fac*-[MnBr(bpy)(CO)₃] was found to be $22.11 \pm 0.01 \text{ min}^{-1}$ (conc.: $1.17 \times 10^{-4} \text{ M}$). It is therefore evident that, much like **1**, the bpy complex *fac*-[MnBr(bpy)(CO)₃] also releases CO when irradiated with light corresponding to the λ_{max} of the low-energy MLCT band. In contrast, the corresponding rhenium complex *fac*-[ReBr(bpy)(CO)₃], with an MLCT band at 391 nm, releases CO only upon exposure to UV light ($\lambda_{\text{max}} \sim 300 \text{ nm}$), with $k_{\text{CO}} = 0.23 \pm 0.02 \text{ min}^{-1}$ (conc.: $7.49 \times 10^{-5} \text{ M}$) in dichloromethane.

Together, these CO photorelease studies indicate that **1–4** are efficient photoCORMs that release CO upon exposure to light. All four complexes display relatively strong absorption bands in the visible region of the spectrum (Figure 4). However, Mn complexes **1** and **2** release CO upon exposure to low-power visible light ($\lambda \geq 500 \text{ nm}$), while the corresponding Re complexes (**3** and **4**) release CO only when exposed to UV light ($\sim 300 \text{ nm}$). It is therefore evident that the presence of strong MLCT bands in the visible region does not translate to sensitivity of a designed photoCORM toward visible light. Labilization of the CO ligand is expected only when significant electron density is transferred from a molecular orbital (MO) with significant metal–CO bonding contribution to a mostly ligand-based MO.^[25] Assessment of such contributions was

therefore necessary to elucidate the photobehavior of the present photoCORMs.

DFT and TDDFT studies

In our previous work, we were able to move the MLCT band(s) of metal–carbonyl complexes through modification of the ligand frame.^[16b,25] Such ligand alteration allowed us to isolate photoCORMs that deliver CO upon exposure to visible light. In the present work, changing the metal center in a set of analogous complexes afforded **1–4**, which exhibit strong MLCT bands in the visible region. The surprising absence of sensitivity toward visible light in case of **3** and **4**, however, indicated that their strong absorptions might not aid in labilization of the Re–CO bonds. We therefore proceeded to examine the nature of the MLCT transitions with the aid of DFT and TDDFT calculations to determine the differences in photosensitivity of the structurally similar complexes **1–4**.

In the initial step, DFT optimization of the structures of the complexes was performed, starting from the X-ray coordinates. The optimized structures of **1–4** agree well with respect to bond lengths and angles as listed in Tables S4 and S5 (Supporting Information). Next, TDDFT calculations were performed to obtain the MO electron densities and the calculated electronic transitions (Table 2). The theoretical spectra of **1–4** agree considerably well with experimental data. The MO contributions that make up the MLCT bands were closely examined, along with the associated UV bands that were experimentally observed to release CO in the case of the Re complexes. Close scrutiny of Table 2 reveals that, in all cases, the lowest-energy band corresponds to the transition from MOs with a strong metal–CO bonding interaction to the LUMO, primarily consisting the ligand– π^* orbital. However, in all cases, the soft auxiliary ligand (Br^- or PPh_3) also makes a significant contributions.

Examination of the MO electron densities of **1** (Table 2) shows that the absorption at 586 nm (responsible for rapid CO release and calculated as 616 nm) arises from a transition (HOMO–1 to LUMO) that is comprised of both MLCT and halide $\rightarrow \pi^*$ (XLCT) character. The HOMO–1 level has 41% $\pi(\text{Mn–CO})$ bonding character, along with 37% Br^- bonding contribution with the rest of the orbital densities in the π -bonding ligand frame. Upon illumination, electron density is transferred to the LUMO consisting of 70% π^* MO of azpy along with 8% Br^- and 18% $\pi(\text{Mn–CO})$ bonding character (Figure 7). Reduction in Mn–CO π -backbonding in such a transfer promotes rapid CO release. In case of **3**, the lowest-energy transition at 530 nm is again a HOMO–1 to LUMO transition. Here, the HOMO–1 consists of 48% $\pi(\text{Re–CO})$ and 22% Br^- bonding character, while the LUMO is composed of 63% π^* MO of azpy, along with 8% Br^- and 27% $\pi(\text{Re–CO})$ bonding character. Despite such similarity in the nature of electronic transition, CO is surprisingly not released from **3** upon illumination at 530 nm (calculated: 517 nm). Clearly, there exists another pathway by which this energy is released by **3** without scission of the Re–CO bond. In rhenium–carbonyl complexes of α -diimine and related ligands, stronger spin-orbit interactions (than those with manganese) are known to lead to better

Table 2. Calculated (TDDFT) energies (*E*), oscillator strengths (*f*), and nature of transitions^[a] in the complexes.

<i>E</i> [nm]	<i>f</i>	Transition
1		
616	0.0099492	$\pi(\text{Mn-CO})\text{-p}(\text{Br}) \rightarrow \pi^*(\text{Py-Azo-Ph})$ (HOMO-1 \rightarrow LUMO)
396	0.0720846	$\pi(\text{Mn-CO})\text{-p}(\text{Br}) \rightarrow \pi^*(\text{Py-Azo-Ph})$
354	0.0797801	$\pi(\text{Ph}) \rightarrow \pi^*(\text{Py-Azo-Ph})$
350	0.1818711	$\pi(\text{Ph})\text{-d}(\text{Mn}) \rightarrow \pi^*(\text{Py-Azo-Ph})$
348	0.0346971	$\text{p}(\text{Br})\text{-}\pi(\text{Mn-CO}) \rightarrow \pi^*(\text{Ph})\text{-}\pi(\text{CO})\text{-d}(\text{Mn})$
336	0.0267677	$\text{p}(\text{Br})\text{-}\pi(\text{Mn-CO}) \rightarrow \pi^*(\text{Py-Ph-Azo})$
331	0.0489395	$\pi(\text{Pyr}) \rightarrow \pi^*(\text{Py-Azo-Ph})$
326	0.0207783	$\pi(\text{Mn-CO})\text{-p}(\text{Br}) \rightarrow \pi^*(\text{Py-Ph-Azo})$
324	0.0239514	$\pi(\text{Mn-CO}) \rightarrow \pi^*(\text{Py-Ph})$
320	0.0283438	$\text{p}(\text{Br})\text{-}\pi(\text{Mn-CO}) \rightarrow \pi^*(\text{Py-Ph-Azo})$
2		
472	0.0134903	$\pi(\text{Mn-PPh}_3\text{-CO}) \rightarrow \pi^*(\text{Py-Azo-Ph})$ (HOMO-4 \rightarrow LUMO)
430	0.0410682	$\pi(\text{Mn-PPh}_3\text{-CO}) \rightarrow \pi^*(\text{Py-Azo-Ph})$
416	0.0233788	$\pi(\text{Mn-PPh}_3)\text{-}\pi(\text{Ph}) \rightarrow \pi^*(\text{Py-Azo-Ph})$
403	0.0198349	$\pi(\text{Mn-PPh}_3) \rightarrow \pi^*(\text{Py-Azo-Ph})$
392	0.0143996	$\pi(\text{Mn-PPh}_3\text{-CO})\text{-}\pi(\text{Py})\text{-}\pi(\text{Ph}) \rightarrow \pi^*(\text{Py-Azo-Ph})$
364	0.1836637	$\pi(\text{Mn-PPh}_3\text{-CO})\text{-}\pi(\text{Ph})\text{-}\pi(\text{Py}) \rightarrow \pi^*(\text{Py-Azo-Ph})$
360	0.0870086	$\pi(\text{Mn-PPh}_3\text{-CO})\text{-}\pi(\text{Ph})\text{-}\pi(\text{Mn-CO}) \rightarrow \pi^*(\text{Py-Azo-Ph})$
328	0.0122870	$\pi(\text{Mn-PPh}_3\text{-CO})\text{-}\pi(\text{Ph}) \rightarrow \text{d}(\text{Mn})\text{-}\pi^*(\text{PPh}_3)\text{-}\pi(\text{CO})\text{-}\pi^*(\text{Py})$
322	0.0217908	$\pi(\text{Mn-CO-PPh}_3)\text{-}\pi(\text{Ph}) \rightarrow \text{d}(\text{Mn})\text{-}\pi^*(\text{PPh}_3)\text{-}\pi(\text{CO})\text{-}\pi^*(\text{Py})$
3		
517	0.0380878	$\pi(\text{Re-CO})\text{-p}(\text{Br}) \rightarrow \pi^*(\text{Py-Azo-Ph})$ (HOMO-1 \rightarrow LUMO)
462	0.0166441	$\pi(\text{Re-CO})\text{-}\pi(\text{Ph}) \rightarrow \pi^*(\text{Py-Azo-Ph})$
380	0.2157011	$\pi(\text{Re-CO})\text{-}\pi(\text{Ph})\text{-}\pi(\text{Py}) \rightarrow \pi^*(\text{Py-Azo-Ph})$
358	0.1375852	$\pi(\text{Re-CO})\text{-p}(\text{Br})\text{-}\pi(\text{Py}) \rightarrow \pi^*(\text{Py-Azo-Ph})$
346	0.0578752	$\pi(\text{Re-CO})\text{-p}(\text{Br})\text{-}\pi(\text{Ph}) \rightarrow \pi^*(\text{Py-Azo-Ph})$
325	0.0286452	$\pi(\text{Py-Azo-Ph}) \rightarrow \pi^*(\text{Py-Azo-Ph})$
291	0.0129495	$\pi(\text{Re-CO})\text{-p}(\text{Br}) \rightarrow \pi^*(\text{Py-Azo-Ph})$
289	0.0376803	$\pi(\text{Re-CO})\text{-p}(\text{Br}) \rightarrow \pi^*(\text{Py-Azo})$
282	0.0247467	$\pi(\text{Re-CO})\text{-p}(\text{Br}) \rightarrow \pi^*(\text{Py-Azo})\text{-}\pi^*(\text{Re-CO})$ (HOMO-1 \rightarrow LUMO + 1/LUMO + 2)
4		
462	0.0233700	$\pi(\text{Re-PPh}_3\text{-CO}) \rightarrow \pi^*(\text{Py-Azo-Ph})$ (HOMO-4 \rightarrow LUMO)
448	0.0176888	$\pi(\text{Re-CO-PPh}_3)\text{-}\pi(\text{Ph}) \rightarrow \pi^*(\text{Py-Azo-Ph})$
424	0.0167423	$\pi(\text{Re-PPh}_3\text{-CO}) \rightarrow \pi^*(\text{Py-Azo-Ph})$
410	0.0139487	$\pi(\text{PPh}_3) \rightarrow \pi^*(\text{Py-Azo-Ph})$
404	0.0280426	$\pi(\text{Re-CO-PPh}_3)\text{-}\pi(\text{Ph}) \rightarrow \pi^*(\text{Py-Azo-Ph})$
390	0.0498241	$\pi(\text{Re-PPh}_3\text{-CO}) \rightarrow \pi^*(\text{Py-Azo-Ph})$
374	0.0103896	$\pi(\text{Re-CO-PPh}_3)\text{-}\pi(\text{Ph}) \rightarrow \pi^*(\text{Py-Azo-Ph})$
372	0.2393981	$\pi(\text{Re-CO-PPh}_3)\text{-}\pi(\text{Ph}) \rightarrow \pi^*(\text{Py-Azo-Ph})$
350	0.0137366	$\pi(\text{Re-PPh}_3\text{-CO}) \rightarrow \pi^*(\text{Py-Azo-Ph})$
275	0.0176668	$\pi(\text{Py-Azo-Ph})\text{-}\pi(\text{Re-CO-PPh}_3) \rightarrow \pi^*(\text{Py-Azo-Ph})$

[a] Orbitals with greater contributions are listed first.

mixing of the low-lying ¹MLCT with ³MLCT, resulting in metal-halide bond homolysis (instead of CO dissociation via a spin-singlet process) upon illumination with light in the visible region.^[32,33] Time-resolved spectroscopic studies also indicated that the halide ligand stays within the solvent cage and rapidly recombines in most cases. Bond restoration depends on the admixture of ¹MLCT with the ³MLCT state of the highly coupled radical pair which, in turn, depends on spin-orbit coupling (prominent in **3**). As a consequence, the energy absorbed through this transition in the visible range is dissipated, with no net CO dissociation from the excited species in these rhenium complexes.^[34] In the present study, **3** therefore exhibits no photorelease of CO when illuminated with 530 nm light.

Further evidence of CO release from the low-lying ¹MLCT transition, in the case of manganese-carbonyl complexes, comes from the loss of CO from *fac*-[MnBr(bpy)(CO)₃] under 420 nm illumination. The HOMO-1 to LUMO transition of this complex is comprised of both MLCT and XLCT character. The HOMO-1 level has 52% $\pi(\text{Mn-CO})$ bonding character, along with 28% Br⁻ bonding contribution, while the LUMO consists of 74% $\pi^*\text{MO}$ of bpy, 8% Br⁻, and 17% $\pi(\text{Mn-CO})$ bonding character. Transfer of electrons during this transition also causes labilization of the Mn-CO bond, much like **1**.

The significant role of the soft auxiliary ligand is evident in the relatively slower photorelease of CO from **2**. Replacement of Br⁻ with PPh₃ (a strong π acceptor) shifts the lowest-energy transition (HOMO-4 \rightarrow LUMO) of **2** to 520 nm. Upon illumination, electron density is transferred from the HOMO-4 orbital, consisting of 28% $\pi(\text{Mn-CO})$ and 38% PPh₃ bonding character, to LUMO, which has 61% $\pi^*\text{MO}$ of azpy along with 18% $\pi(\text{Mn-CO})$ and 18% PPh₃ bonding character. Overall, this transition transfers more electron density from the PPh₃ ligand, which competes with CO in terms of π -backbonding. As a consequence, weakening of the Mn-CO bond is not as severe as in the case of **1**, in which Br⁻ acts more as a donor ligand.

Finally, in the case of **3**, absorption of \sim 300 nm light transfers electron density from HOMO-1 to LUMO + 1 (consisting of 69% $\pi^*\text{MO}$ of azpy, 26% $\pi(\text{Re-CO})$, and 5% Br⁻) and LUMO + 2 (consisting of 31% $\pi^*\text{MO}$ of azpy, 63% $\pi^*(\text{Re-CO})$ and 4% Br⁻, Figure 7). Despite intersystem crossing to their respective non-dissociative triplet states, the potential energy surfaces are somewhat dissociative, presumably due to avoiding crossing with a higher ¹LF state along the reaction coordinate.^[35] As a consequence, minor Re-CO labilization is observed when **3** is exposed to \sim 300 nm light, and the rate of CO photorelease from **3** is \sim 500-fold slower than that noted with **1** under similar conditions.

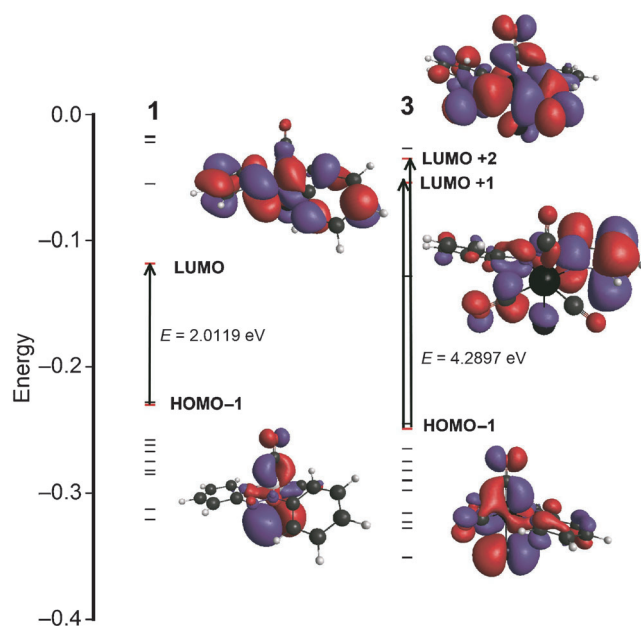


Figure 7. Calculated energy diagram of **1** and **3** (left to right). The most prominent MOs involved with transitions under the band associated with CO release and their compositions are shown.

Conclusions

Together, results of the present work demonstrate that even though two very structurally similar metal–carbonyl complexes (**1** and **3**) exhibit strong MLCT bands in the visible region, the rhenium congener fails to release CO upon illumination with visible light. As a consequence, despite higher stability in biological media, **3** can hardly be employed as a photoCORM under the control of visible/near-IR light. To date, most of the photochemical studies on rhenium–carbonyl complexes with α,α' -diimine ligands have been performed with UV light.^[34] The recent report on the use of $[\text{Re}(\text{bpy})(\text{CO})_3(\text{thp})]^+$ as a photoCORM also employed UV light for CO release.^[14] In general, these rhenium(I) complexes are pale in color (yellow to light orange) and exhibit no strong absorption in the visible range.^[36] We now show that although proper choice of ligands in complexes like **3** could lead to strong absorption in the visible region (deep purple in color), CO release is not observed when the complex is exposed to light of similar wavelengths. The energy absorbed by **3** in this region is dissipated through pathways that do not initiate CO release. It therefore appears that the potential of rhenium–carbonyl complexes as photoCORMs in the visible region is rather limited relative to that of the manganese congeners. Indeed, photoCORMs that exhibit CO release under visible light have so far been centered around elements of the first transition row (Mn and Fe).^[10,12] Our results also indicate that soft halide ligands such as Br^- aid in red-shifting the MLCT bands of such complexes^[23,25] and in promoting faster CO release through mixing of the XLCT and MLCT transitions. We anticipate that these findings will provide helpful tips in the future quest for photoactive CO-donating drugs that could be triggered by visible/near-IR light.

Experimental Section

$[\text{Mn}(\text{CO})_5\text{Br}]$ and $\text{AgClO}_4 \cdot \text{H}_2\text{O}$ were purchased from Alpha Aesar, and $[\text{Re}(\text{CO})_5\text{Br}]$ was procured from Strem Chemical, Inc. The lattice water molecules of $\text{AgClO}_4 \cdot \text{H}_2\text{O}$ was removed via trituration with CH_3CN several times prior to use. The ligand 2-phenylazopyridine (azpy) was synthesized by following a reported procedure.^[20] Solvents were purified and/or dried by standard techniques prior to use. ^1H NMR spectra were recorded at 298 K on a Varian Unity Inova 500 MHz instrument. A PerkinElmer Spectrum-One FT-IR was employed to monitor IR spectra, while the UV/Vis spectra were obtained with a Varian Cary 5000 UV/Vis-NIR spectrophotometer. Microanalyses (C, H, N) were performed using a PerkinElmer 2400 Series II elemental analyzer. Horse heart myoglobin (Mb) was purchased from Sigma–Aldrich and used as received.

Caution! Transition metal perchlorates should be prepared in small quantities and handled with great caution, as metal perchlorates may explode upon heating.

Synthesis of complexes

[MnBr(azpy)(CO)₃] (1): A batch of 100 mg (0.36 mmol) of $[\text{MnBr}(\text{CO})_5]$ was mixed with 80 mg (0.44 mmol) azpy in 20 mL CH_2Cl_2 , and the reaction mixture was stirred for 24 h at room temperature. During this time, the dark blue solution was covered with aluminum foil to prevent exposure from ambient light. After 24 h, the solvent was removed to obtain a dark blue solid, which was washed thoroughly with hexanes. Dark blocks of **1** in good yield (90 mg, 63%) were obtained through recrystallization by layering hexanes over its CH_2Cl_2 solution. ^1H NMR (500 MHz, CD_3CN): $\delta = 9.23$ (d, 1H), 8.66 (d, 1H), 8.33 (t, 1H), 7.87 (d, 2H), 7.74 (t, 1H), 7.68 ppm (d, 3H); IR (KBr): $\tilde{\nu}_{\text{CO}} = 2040, 1960, \text{ and } 1940$, $\tilde{\nu}_{\text{N=N}} = 1370 \text{ cm}^{-1}$; UV/Vis (CH_2Cl_2), $\lambda_{\text{max}}(\epsilon) = 330$ (13000), 586 (3900); Anal. calcd for $\text{C}_{14}\text{H}_9\text{N}_3\text{O}_3\text{BrMn}$: C 41.83, H 2.26, N 10.46, found: C 41.60, H 2.41, N 10.52.

[Mn(azpy)(CO)₃(PPh₃)](ClO₄) (2): A batch of 33 mg (0.16 mmol) of AgClO_4 was added to a solution of 50 mg (0.12 mmol) of $[\text{MnBr}(\text{azpy})(\text{CO})_3]$ in 10 mL of THF, and the resulting blue reaction mixture was stirred for 3 h in the dark, resulting in a purple solution. The precipitate of AgBr was then filtered with a wet Celite pad, and the filtrate was evaporated to dryness. The solid residue was washed with hexanes. Next, a solution of 66 mg (0.25 mmol) of PPh_3 in 10 mL of CH_2Cl_2 was added to the residue, and the reaction mixture was stirred for 24 h. The reaction flask in all steps was covered with aluminum foil. Finally, the solvent was removed, and the residue was washed thoroughly with benzene to obtain **2** as an orange–red solid in moderate yield (38 mg, 45%): ^1H NMR (500 MHz, CDCl_3): $\delta = 8.59$ (m), 8.43 (m), 7.67 (m), 7.52 (m), 7.42 (m), 7.26 (m), 7.06 (m), and 5.30 ppm (m); IR (KBr): $\tilde{\nu}_{\text{CO}} = 2045, 1980, \text{ and } 1950$, $\tilde{\nu}_{\text{N=N}} = 1370$, $\tilde{\nu}_{\text{ClO}_4} = 1090 \text{ cm}^{-1}$; UV/Vis (CH_2Cl_2): $\lambda_{\text{max}}(\epsilon) = 370$ (11500), 520 (4050); Anal. calcd for $\text{C}_{32}\text{H}_{24}\text{N}_3\text{O}_7\text{PMn}$: C 56.20, H 3.54, N 6.15, found: C 55.95, H 3.62, N 6.10.

[ReBr(azpy)(CO)₃] (3): A mixture of 74 mg (0.18 mmol) of $[\text{ReBr}(\text{CO})_5]$ and 40 mg (0.22 mmol) of azpy in 30 mL of benzene was stirred at reflux for 3 h. The volume of the deep-purple solution was then decreased to ~ 5 mL, and it was stored at 4°C for 6 h. The resulting purple solid was collected by filtration and washed thoroughly with hexanes. Block-shaped crystals were obtained through recrystallization by layering hexanes over a CH_2Cl_2 solution to afford **3** in good yield (70 mg, 72%): ^1H NMR (500 MHz, CDCl_3): $\delta = 9.08$ (d, 1H), 8.63 (d, 1H), 8.25 (t, 1H), 7.97 (d, 2H), 7.64 (t, 2H), 7.59 ppm (t, 2H); IR (KBr): $\tilde{\nu}_{\text{CO}} = 2030, 1930, \text{ and } 1920$, $\tilde{\nu}_{\text{N=N}} =$

$\nu_{\text{N}} = 1370 \text{ cm}^{-1}$; UV/Vis (CH_2Cl_2): $\lambda_{\text{max}}(\epsilon) = 370$ (12400), 530 (4600); Anal. calcd for $\text{C}_{14}\text{H}_9\text{N}_3\text{O}_3\text{BrRe}$: C 31.55, H 1.70, N 7.89, found: C 31.60, H 1.57, N 7.82.

[Re(azpy)(CO)₃(PPh₃)](ClO₄) (4): A mixture of 51 mg (0.25 mmol) of AgClO_4 and 100 mg (0.19 mmol) of $[\text{ReBr}(\text{azpy})(\text{CO})_3]$ was dissolved in 10 mL of THF, and the purple solution was stirred at reflux for 3 h, at which point the color changed to dark orange. The solid AgBr was then filtered on a wet Celite pad, and the filtrate was evaporated to dryness. Next, the orange residue was dissolved in 10 mL of chloroform along with 65 mg (0.25 mmol) of PPh_3 , and the reaction mixture was stirred at reflux for 8 h. The solvent was then evaporated under reduced pressure, and the resulting solid was dissolved in 5 mL of CH_2Cl_2 and subjected to column chromatography (silica gel, 60–100 mesh). Initially, the column was eluted with benzene (10 mL \times 3) to remove any trace of the parent compound. Finally, the deep orange–red band was eluted using a mixture of benzene and CH_3CN (25:2, v/v) in which a small amount of $(\text{Et}_4\text{N})\text{ClO}_4$ was dissolved. The eluate was evaporated to dryness and recrystallized by layering hexanes over its solution in CH_2Cl_2 . Orange needles of **4** were obtained in moderate yield (85 mg, 55%): $^1\text{H NMR}$ (500 MHz, CDCl_3): $\delta = 8.65$ (d, 1H), 8.57 (d, 1H), 8.49 (t, 1H), 7.68 (m, 6H), 7.55 (m, 4H), 7.40 (t, 3H), 7.28 (ir, 3H), 7.04 ppm (t, 5H); IR (KBr): $\tilde{\nu}_{\text{CO}} = 2050, 1970, \text{ and } 1940$, $\tilde{\nu}_{\text{N}=\text{N}} = 1370$, $\tilde{\nu}_{\text{ClO}_4} = 1090 \text{ cm}^{-1}$; UV/Vis (CH_2Cl_2): $\lambda_{\text{max}}(\epsilon) = 390$ (12400), 460 (6100); Anal. calcd for $\text{C}_{32}\text{H}_{24}\text{N}_3\text{O}_7\text{PClRe}$: C 47.15, H 2.97, N 5.16, found: C 47.25, H 2.78, N 5.12.

[MnBr(bpy)(CO)₃]: A mixture of 100 mg (0.36 mmol) of $[\text{MnBr}(\text{CO})_3]$ and 56 mg (0.36 mmol) of bpy in 20 mL of benzene was stirred at reflux for 2 h. The yellow-orange solution was then evaporated to dryness, and the residue was washed thoroughly with hexanes. The yellow solid was finally recrystallized by layering the hexanes over its CH_2Cl_2 solution. After 4 days, block-shaped orange crystals of $[\text{MnBr}(\text{bpy})(\text{CO})_3]$ were obtained in good yield (95 mg, 70%): $^1\text{H NMR}$ (500 MHz, CDCl_3): $\delta = 9.23$ (1H), 8.34 (1H), 8.12 (1H), 7.62 ppm (2H); IR (KBr): $\tilde{\nu}_{\text{CO}} = 2023, 1945, \text{ and } 1925 \text{ cm}^{-1}$; UV/Vis (CH_2Cl_2): $\lambda_{\text{max}}(\epsilon) = 300$ (10500), 420 (1100); Anal. calcd for $\text{C}_{13}\text{H}_8\text{N}_2\text{O}_3\text{BrMn}$: C 41.59, H 2.13, N 7.47, found: C 41.83, H 2.12, N 7.44.

[ReBr(bpy)(CO)₃]: This complex was obtained in good yield (93 mg, 75%) by following a similar procedure as for $[\text{MnBr}(\text{bpy})(\text{CO})_3]$ except with a longer reflux time (7 h): $^1\text{H NMR}$ (500 MHz, CDCl_3): $\delta = 9.11$ (d, 1H), 8.20 (d, 1H), 8.08 (t, 1H), 7.56 ppm (t, 2H); IR (KBr): $\tilde{\nu}_{\text{CO}} = 2012, 1905, 1882 \text{ cm}^{-1}$; UV/Vis (CH_2Cl_2): $\lambda_{\text{max}}(\epsilon) = 300$ (19400), 400 (3600); Anal. calcd for $\text{C}_{13}\text{H}_8\text{N}_2\text{O}_3\text{BrRe}$: C 30.81, H 1.58, N 5.53, found: C 31.03, H 1.49, N 5.41.

Crystallography: Single crystals of **1–4** were obtained by layering hexanes over their solutions in CH_2Cl_2 . Data were collected on a Bruker APEX II single crystal X-ray diffractometer with graphite monochromated $\text{MoK}\alpha$ radiation ($\lambda = 0.71073 \text{ \AA}$) by ω -scan technique in the range of $3 \geq 2\theta \geq 55^\circ$ for complex **1**, $3 \geq 2\theta \geq 57^\circ$ for complex **2**, and $3 \geq 2\theta \geq 56^\circ$ for complexes **3** and **4**. All data were corrected for Lorentz polarization and absorption.^[37] The metal atoms were located from the Patterson maps, and the rest of the non-hydrogen atoms emerged from successive Fourier syntheses. The structures were refined by the full-matrix least-squares procedure on F^2 . All non-hydrogen atoms were refined anisotropically. All hydrogen atoms were included in calculated positions. The absorption corrections were done using SADABS. Calculations were performed using the SHELXTL ver. 6.14 software package.^[38] Crystallographic data are presented in Table S1 (Supporting Information).

Photolysis experiment: For visible light irradiation, an IL410 illumination system (Electro FiberOptics Corporation; power: 10–15 mW cm^{-2}) was used. The UV light source employed in this study was a UV-Transilluminator (UVP Inc.) with peak intensity at 305 nm (power: 5 mW cm^{-2}). Apparent rates of CO release (k_{CO}) were followed at an appropriate wavelength for each complexes, and $\ln[\text{concentration}]$ versus time (T) plots were generated. The myoglobin (Mb) assay was carried out following standard protocols.^[15]

DFT and TDDFT studies: Density functional theory (DFT) and time-dependent density functional theory (TDDFT) studies were performed with the aid of the PC-GAMESS program^[39] using the hybrid functionals PBE0 and PBE1PW91 for Mn and Re complexes, respectively. Optimizations for the Mn atom were performed by employing the LANL2DZ basis set in conjunction with effective core potential (ECP). For the Re atom, a valence double zeta (cc-pVDZ-PP) basis set was used. The Pople 6-311G* split-valence triple- ζ basis set with polarization was used for Br, while for all other atoms, the 6-31G* basis set was employed with valence double- ζ polarization (VDZP). The X-ray crystal structure coordinates of complexes **1–4** were used as a starting point for the gas-phase geometry optimization of the low spin ($S=0$) ground states. TDDFT was used to calculate the electronic transitions and associated energies. Transitions with oscillator strengths above 0.0099 were then taken for analysis. For calculations on **1–4**, the 40 lowest-energy electronic excitations were calculated. For each Re compound, solvent effects were added using the polarized continuum model (PCM)^[40] using EtOH as the solvent. The calculated molecular orbitals were visualized using MacMolPlt.^[41]

CCDC 977174, 977175, and 977176 contain the supplementary crystallographic data for this paper. These data can be obtained free of charge from the Cambridge Crystallographic Data Centre via www.ccdc.cam.ac.uk/data_request/cif.

Acknowledgements

Financial support from the NSF (grant DMR-1105296) is gratefully acknowledged.

Keywords: carbonyl ligands · drug design · manganese · photolysis · rhenium

- [1] R. Tenhunen, H. S. Marver, R. Schmid, *Proc. Natl. Acad. Sci. USA* **1968**, *61*, 748–755.
- [2] a) R. Motterlini, L. E. Otterbein, *Nat. Rev. Drug Discovery* **2010**, *9*, 728–743; b) J. McDaid, K. Yamashita, A. Chora, R. Öllinger, T. B. Strom, X. C. Li, F. H. Bach, M. P. Soares, *FASEB J.* **2005**, *19*, 458–460; c) R. Song, Z. Zhou, P. K. M. Kim, R. A. Shapiro, F. Liu, C. Ferran, A. M. K. Choi, L. E. Otterbein, *J. Biol. Chem.* **2004**, *279*, 44327–44334.
- [3] S. W. Ryter, A. M. K. Choi, *Korean J. Intern. Med.* **2013**, *28*, 123–140.
- [4] K. Sato, J. Balla, L. Otterbein, R. N. Smith, S. Brouard, Y. Lin, E. Csizmadia, J. Sevigny, S. C. Robson, G. Vercellotti, A. M. Choi, F. H. Bach, M. P. Soares, *J. Immunol.* **2001**, *166*, 4185–4194.
- [5] B. E. Mann, R. Motterlini, *Chem. Commun.* **2007**, 4197–4208.
- [6] R. Alberto, R. Motterlini, *Dalton Trans.* **2007**, 1651–1660.
- [7] T. R. Johnson, B. E. Mann, J. E. Clark, R. Foresti, C. J. Green, R. Motterlini, *Angew. Chem. Int. Ed.* **2003**, *42*, 3722–3729; *Angew. Chem.* **2003**, *115*, 3850–3858.
- [8] a) C. C. Romão, W. A. Blätter, J. D. Seixas, G. J. L. Bernardes, *Chem. Soc. Rev.* **2012**, *41*, 3571–3583; b) T. Santos-Silva, A. Mukhopadhyay, J. D. Seixas, G. J. L. Bernardes, C. C. Romão, M. J. Romão, *J. Am. Chem. Soc.* **2011**, *133*, 1192–1195; c) T. R. Johnson, B. E. Mann, I. P. Teasdale, H. Adams, R. Foresti, C. J. Green, R. Motterlini, *Dalton Trans.* **2007**, 1500–1508.

- [9] R. Alberto, *Eur. J. Inorg. Chem.* **2009**, 21–31.
- [10] M. A. Gonzales, P. K. Mascharak, *J. Inorg. Biochem.* **2014**, *133*, 127–135.
- [11] R. D. Rimmer, A. E. Pierri, P. C. Ford, *Coord. Chem. Rev.* **2012**, *256*, 1509–1519.
- [12] U. Schatzschneider, *Inorg. Chim. Acta* **2011**, *374*, 19–23.
- [13] a) B. Arregui, B. López, M. G. Salom, F. Valero, C. Navarro, F. J. Fenoy, *Kidney Int.* **2004**, *65*, 564–574; b) P. Koneru, C. W. Leffler, *Am. J. Physiol. Heart Circ. Physiol.* **2004**, *286*, H304–H309; c) R. Motterlini, J. E. Clark, R. Foresti, P. Sarathchandra, B. E. Mann, C. J. Green, *Circ. Res.* **2002**, *90*, E17–E24.
- [14] A. E. Pierri, A. Pallaoro, G. Wu, P. C. Ford, *J. Am. Chem. Soc.* **2012**, *134*, 18197–18200.
- [15] J. Niesel, A. Pinto, H. W. P. N'Dongo, K. Merz, I. Ott, R. Gust, U. Schatzschneider, *Chem. Commun.* **2008**, 1798–1800.
- [16] a) S. J. Carrington, I. Chakraborty, J. R. Alvarado, P. K. Mascharak, *Inorg. Chim. Acta* **2013**, *407*, 121–125; b) M. A. Gonzalez, S. J. Carrington, I. Chakraborty, M. M. Olmstead, P. K. Mascharak, *Inorg. Chem.* **2013**, *52*, 11320–11331.
- [17] a) C. Bischof, T. Joshi, A. Dimri, L. Spiccia, U. Schatzschneider, *Inorg. Chim. Acta* **2013**, *52*, 9297–9308; b) P. Govender, S. Pai, U. Schatzschneider, G. S. Smith, *Inorg. Chem.* **2013**, *52*, 5470–5478; c) G. Dördelmann, T. Meinhardt, T. Sowik, A. Krueger, U. Schatzschneider, *Chem. Commun.* **2012**, *48*, 11528–11530; d) P. C. Kunz, W. Huber, A. Rojas, U. Schatzschneider, B. Spingler, *Eur. J. Inorg. Chem.* **2009**, 5358–5366.
- [18] J. D. Seixas, A. Mukhopadhyay, T. Santos-Silva, L. E. Otterbein, D. J. Gallo, S. S. Rodrigues, B. H. Guerreiro, A. M. L. Gonçalves, N. Penacho, A. R. Marques, A. C. Coelho, P. M. Reis, M. J. Romão, C. C. Romão, *Dalton Trans.* **2013**, *42*, 5985–5998.
- [19] W. Q. Zhang, A. C. Whitwood, I. J. S. Fairlamb, J. M. Lynam, *Inorg. Chem.* **2010**, *49*, 8941–8952.
- [20] R. D. Rimmer, H. Richter, P. C. Ford, *Inorg. Chem.* **2010**, *49*, 1180–1185.
- [21] D. E. Bikiel, E. G. Solveyra, F. D. Salvo, H. M. S. Milagre, M. N. Eberlin, R. S. Corrêa, J. Ellena, D. A. Estrin, F. Doctorovich, *Inorg. Chem.* **2011**, *50*, 2334–2345.
- [22] F. Zobi, A. Degonda, M. C. Schaub, A. Y. Bogdanova, *Inorg. Chem.* **2010**, *49*, 7313–7322.
- [23] S. J. Carrington, I. Chakraborty, P. K. Mascharak, *Chem. Commun.* **2013**, *49*, 11254–11256.
- [24] F. Zobi, L. Quaroni, G. Santoro, T. Zlateva, O. Blacque, B. Sarafimov, M. C. Schaub, A. Y. Bogdanova, *J. Med. Chem.* **2013**, *56*, 6719–6731.
- [25] M. A. Gonzalez, S. J. Carrington, N. L. Fry, J. L. Martinez, P. K. Mascharak, *Inorg. Chem.* **2012**, *51*, 11930–11940.
- [26] K. Koike, N. Okoshi, H. Hori, K. Takeuchi, O. Ishitani, H. Tsubaki, I. P. Clark, M. W. George, F. P. A. Johnson, J. J. Turner, *J. Am. Chem. Soc.* **2002**, *124*, 11448–11455.
- [27] A. Mostad, C. Romming, *Acta Chem. Scand.* **1971**, *25*, 3561–3568.
- [28] S. J. Dougan, M. Melchart, A. Habtemariam, S. Parsons, P. J. Sadler, *Inorg. Chem.* **2006**, *45*, 10882–10894.
- [29] B. J. Liddle, S. V. Lindeman, D. L. Reger, J. R. Gardinier, *Inorg. Chem.* **2007**, *46*, 8484–8486.
- [30] H. Tsubaki, S. Tohyama, K. Koike, H. Saitoh, O. Ishitani, *Dalton Trans.* **2005**, 385–395.
- [31] A. Vlček, Jr., *Coord. Chem. Rev.* **2002**, *230*, 225–242.
- [32] C. Daniel, D. Guillaumont, C. Ribbing, B. Minaev, *J. Phys. Chem. A* **1999**, *103*, 5766–5772.
- [33] a) A. Vogler, H. Kunkely, *Coord. Chem. Rev.* **2000**, *200–202*, 991–1008; b) D. J. Stufkens, *Coord. Chem. Rev.* **1990**, *104*, 39–112.
- [34] a) S. Sato, A. Sekine, Y. Ohashi, O. Ishitani, A. M. Blanco-Rodriguez, A. Vlček, Jr., T. Unno, K. Koike, *Inorg. Chem.* **2007**, *46*, 3531–3540; b) M. Wrighton, D. L. Morse, *J. Am. Chem. Soc.* **1974**, *96*, 998–1003.
- [35] I. R. Farrell, P. Matousek, M. Towrie, A. W. Parker, D. C. Grills, M. W. George, A. Vlček, Jr., *Inorg. Chem.* **2002**, *41*, 4318–4323.
- [36] R. A. Kirgan, B. P. Sullivan, D. P. Rillema, *Top. Curr. Chem.* **2007**, *281*, 45–100.
- [37] A. C. T. North, D. C. Philips, F. S. Mathews, *Acta Crystallogr.* **1968**, *24*, 351–359.
- [38] G. M. Sheldrick, SHELXTL ver. 6.14, Bruker Analytical X-ray Systems, Madison, WI (USA), **2000**.
- [39] A. V. Nemukhin, B. L. Grigorenko, A. A. Granovsky, *Moscow Univ. Chem. Bull.* **2004**, *45*, 75–102.
- [40] S. Miertus, E. Scrocco, J. Tomasi, *Chem. Phys.* **1981**, *55*, 117–120.
- [41] M. P. Waller, H. Braun, N. Hojdis, M. Buhl, *J. Chem. Theory Comput.* **2007**, *3*, 2234–2242.

Received: February 3, 2014

Published online on April 23, 2014